Ionic Conductivity of Doped NaCl Crystals

R. W. DREYFUS AND A. S. NOWICK
International Business Machines Corporation, Yorktown Heights, New York

(Received December 26, 1961)

A detailed study is made of the "conductivity plot" ($\log\sigma T$ vs T^{-1}) for the dc ionic conductivity, σ, of NaCl crystals doped with various divalent cation impurities. This plot, when examined over a range from the melting point down to -35°C, divides itself into a number of distinct regions. Below the intrinsic range is the region in which the cation-vacancy concentration is equal to the impurity concentration. Below this range the plot steepens due to the occurrence of vacancy-impurity association, after which it again steepens (for slowly cooled samples) due to impurity precipitation. At still lower temperatures, (below about 100°C), the plot returns to a slope characteristic of the association reaction. Finally, by "quenching" a sample to -60°C (at 30°C/min), the association reaction may be frozen and an abnormally high conductivity observed below 0°C. From an analysis of the data for quenched samples, a value for the activation energy for motion of a cation vacancy in NaCl, of $0.79_6\pm0.02$ ev, is obtained. The isothermal annealing of the quenched-in vacancies is also studied and found to obey essentially first-order kinetics, rather than the second-order kinetics characteristic of direct recombination.

1. INTRODUCTION

THE ionic conductivity of alkali halide crystals of the NaCl type occurs predominantly through the motion of vacancies.[1] Measurements of mass transport during conduction have further established that, except near the melting point, the current is carried almost entirely by the motion of the cations.[2] Accordingly, the cation vacancy is regarded as the mobile charge carrier. The electrical conductivity, σ, is then given by the following expression[1]:

$$\sigma=ne\mu=\left(\frac{4e^2a^2\nu_0}{kT}\right)n\exp(-\epsilon_m/kT), \tag{1}$$

where n is the concentration of cation vacancies, μ is the mobility of the vacancy, a is the distance between the nearest-neighbor cation and anion (one-half the lattice parameter), ϵ_m is the activation energy for motion of a cation vacancy, ν_0 is a frequency factor (which contains an effective lattice vibration frequency multiplied by an entropy factor), and e and kT have their usual meanings. The expression for the mobility, which results in the right-hand side of Eq. (1), is derived from the fact that the mean time, τ_v, between vacancy jumps, is given by

$$\tau_v^{-1}=12\nu_0\exp(-\epsilon_m/kT). \tag{2}$$

Here the factor 12 appears because of the 12 nearest-neighbor sites into which the vacancy may go.

Equation (1) suggests that data for conductivity as a function of temperature be plotted as $\log\sigma T$ vs T^{-1}, a scheme which we will call the "conductivity plot." If the slope of such a plot is set equal to $-\epsilon/2.303k$, the quantity ϵ, which represents an *effective activation energy*,[3] is equal to ϵ_m plus an energy associated with the temperature dependence of n. A schematic diagram of the conductivity plot, showing the three regions which have been definitely established, is presented in Fig. 1. In region I, which is known as the "intrinsic" region, n is the equilibrium concentration of Schottky defects in the lattice, given by[1]

$$n/N\propto\exp(-\epsilon_s/2kT)\quad\text{(region I)}, \tag{3}$$

where ϵ_s is the energy of formation of a Schottky pair, and N is the concentration of cation lattice sites. Combining Eqs. (3) and (1) shows that the effective activation energy, $\epsilon_{\rm I}$, for region I is given by

$$\epsilon_{\rm I}=\epsilon_m+\tfrac{1}{2}\epsilon_s. \tag{4}$$

A compilation of experimental results for NaCl by various authors gives[4] $\epsilon_{\rm I}$ as 1.86 ± 0.03 ev.

For crystals of ordinary purity, the cation vacancies below about 400°C have a different origin. These are the vacancies which accompany divalent metallic impurity ions (designated M^{++}) so as to maintain the electrical neutrality of the crystal. When the number of vacancies introduced by divalent cation impurities exceeds the number produced thermally, the conductivity breaks into region II of Fig. 1. In this region, the concentration of cation vacancies is a constant, equal to the total concentration of divalent metallic impurities, $N_M{}^0$; from Eq. (1), therefore, the effective activation energy, $\epsilon_{\rm II}$, for this region is simply equal to ϵ_m. Thus:

$$\left.\begin{aligned} n&=N_M{}^0=\text{const}\\ \epsilon_{\rm II}&=\epsilon_m\end{aligned}\right\}\ \text{(region II)}. \tag{5}$$

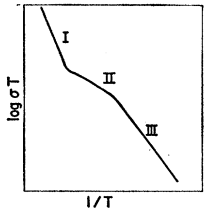

FIG. 1. Schematic drawing of the variation of $\log\sigma T$ with $1/T$ for an NaCl crystal, showing regions which have been reported.

[1] A. B. Lidiard, in *Handbuch der Physik*, edited by S. Flügge (Springer-Verlag, Berlin, 1957), Vol. 20, p. 246.
[2] C. Tubandt, H. Reinhold, and G. Liebold, Z. anorg. u. allgem. Chem. **197**, 225 (1931).
[3] Some authors report, for the effective activation energy, the negative slope of the plot of $\log\sigma$ vs T^{-1} multiplied by $2.303k$. This quantity, which is smaller by kT than the one defined above (where T is the mean temperature of the range studied), is less meaningful than the present definition.
[4] R. W. Dreyfus and A. S. Nowick, J. Appl. Phys. Suppl. **33**, 473 (1962).

Based on the above considerations, one could hope to determine ϵ_s and ϵ_m separately from a knowledge of ϵ_{I} and ϵ_{II}. The difficulty in obtaining such values has been in part due to the fact that region II extends over only a limited range of conductivity, and also to the possibility that Debye-Hückel type interactions[1] modify the interpretation. A wide discrepancy in the values of ϵ_m for NaCl exists among different authors, ranging from 0.72 ev.[5] to 0.85 ev.[6] (The latter value of Etzel and Maurer, which has been the most widely accepted one, was actually obtained by analyzing the dependence of conductivity on Cd^{++} concentration in the range between 250° and 400°C.) Two reasons have been given[1] for the failure of region II to continue to low temperatures. The first is the tendency of the oppositely charged M^{++} ion and the cation vacancy to associate to form a neutral complex. The second is the precipitation of M^{++} ions at temperatures where their concentration in solution begins to exceed the solubility limit. Both of these effects result in a decrease in n below the value $N_M{}^0$, and therefore can account for the onset of region III, as shown in Fig. 1. The separation of the two effects, however, has not been carried out in an unambiguous manner.

The effect of the association reaction on the conductivity is easily calculated for dilute solutions. The reaction itself may be expressed in the form

$$M+V \rightleftarrows MV, \tag{6}$$

where M and V represent the metallic impurity ion and the cation vacancy, respectively, and MV, the associated complex. The binding energy of the complex is known from theoretical considerations[7] to be $\sim$0.4 ev. Application of elementary statistical mechanics to this reaction gives

$$\frac{N_{MV}N}{nN_M}=K_1{}^{-1}=\sum_l z_l \exp(+\epsilon_l/kT), \tag{7}$$

where N_{MV} is the concentration of the MV complex, N_M is the concentration of isolated impurity ions, the subscript l refers to the various bound states in which the pair may be found (e.g., nearest neighbor, next-nearest neighbor, etc.), while z_l and ϵ_l are the number of possible configurations and the binding energy, respectively, for state l. [The definition of the ϵ_l's as *binding energies* is the reason for the appearance of the + sign in the exponent of Eq. (7).] In most cases the values of ϵ_l for one or two of the closest bound states is distinctly larger than that for the higher states, so that the summation is reasonably replaced by a single term, $z_A \exp(+\epsilon_A/kT)$. The following auxiliary relations are added to Eq. (7):

$$n=N_M, \tag{8}$$

$$N_M+N_{MV}=N_M{}^0. \tag{9}$$

The first of these expresses the condition of charge neutrality, while the second expresses the conservation of the added impurity. Equations (7), (8), and (9) may then be solved for n. Of particular interest is the solution at the lower temperatures, where association is almost complete (i.e., $n \ll N_M{}^0$). The result obtained is

$$n^2=N_M{}^0NK_1 \sim (N_M{}^0N/z_A)\exp(-\epsilon_A/kT). \tag{10}$$

If region III is due to this association reaction, then combining Eq. (10) with (1) gives for the effective activation energy

$$\epsilon_{\mathrm{III}}=\epsilon_m+\tfrac{1}{2}\epsilon_A. \tag{11}$$

This interpretation of region III in terms of association, without considering precipitation, is subject to question, however. In particular, extensive evidence for precipitation has appeared from electron spin resonance[8] as well as from x-ray observations.[9]

The purpose of the present work is twofold. First, it is desired to obtain a better understanding of region III of the conductivity plot, and in particular, to separate out the roles of precipitation and of association in reducing the cation vacancy concentration. Second, it is desired to establish the value of ϵ_m for NaCl to a greater degree of certainty than that to which it is presently known. With an accurate knowledge of ϵ_m, it becomes possible to obtain a reliable value for ϵ_s from the data for the intrinsic range [see Eq. (4)] and for ϵ_A in such a range as Eq. (11) may apply. It is also necessary to know ϵ_m in order to evaluate rates of vacancy migration, as given by Eq. (2), so that it becomes possible to make a better estimate of the kinetics of defect reactions at a given temperature. In order to accomplish this second objective, the authors propose to carry out the following experiment on impurity-doped NaCl crystals. A sample will be rapidly cooled from region III to below room temperature. If region III involves the association reaction (6), it should be possible to quench in a nonequilibrium degree of dissociation, and, therefore, a nonequilibrium excess of cation vacancies. Under these conditions n will again be equal to a constant, so that a value of ϵ equal to ϵ_m should be obtainable from the conductivity plot. Finally, the kinetics of the elimination of the excess conductivity may be observed.

In order to carry out the above program, it is desirable to attain a sensitivity in the conductivity readings which will be sufficient to permit measurements to temperatures well below room temperature. For this purpose dc techniques, which utilize electrometer circuitry, appear to be most suitable. In view of the fact that the interpretation of dc measurements has been the subject of some degree of controversy, however, it is first necessary

[5] Y. Haven, *Report of the Conference on Defects in Crystalline Solids* (The Physical Society, London, 1955), p. 261.
[6] H. Etzel and R. Maurer, J. Chem. Phys. **18**, 1003 (1950).
[7] F. Bassani and F. Fumi, Nuovo cimento **11**, 274 (1954).
[8] G. D. Watkins, Phys. Rev. **113**, 79 (1959).
[9] K. Suzuki, J. Phys. Soc. Japan, **16**, 67 (1961); **13**, 179 (1958); **10**, 794 (1955).

to discuss the question of how to obtain the true ionic conductivity from a dc experiment. The source of confusion in such an experiment is the fact that the measured current density, under a given electric field applied at $t=0$, is time dependent. Thus the conductivity may be regarded as a time dependent quantity which decreases from a value σ_0 at $t=0$ to a final (or "steady-state") value, σ_∞, as $t\rightarrow\infty$. It has commonly been supposed, since the work of Joffé,[10] that this time dependent polarization effect was due to inability of the moving charges to be discharged at the electrodes, with the resulting buildup of space charge in the crystal. According to this interpretation, the quantity σ_0 is the "true" conductivity, i.e., the quantity which should be used in Eq. (1). Recent work of Sutter[11] has shown, however, that this interpretation is not valid, at least for sodium chloride crystals. This conclusion was arrived at from the fact that the nonlinear effects predicted for the electrode blocking mechanism[12] were not found; rather Ohm's law and the principle of superposition of currents were strictly obeyed. Sutter also carried out other experiments, such as soft x-ray irradiation of the region of the crystal just below the electrodes, which appear to contradict the suggestion of space charge buildup. Earlier probe measurements[13] also gave no indication of large electric fields due to space charge near the surfaces of alkali halide crystals. For these reasons, the present experiments will report for the conductivity, σ, the value obtained from the final current density in dc measurements. The time-dependent polarization, which is being ignored in the present paper, may originate in a number of different mechanisms. One of these, which has been well established[14] for the region below 0°C, is the reorientation of MV complexes under the influence of the applied field. Other higher temperature mechanisms may involve dislocation effects.

2. EXPERIMENTAL ARRANGEMENT

The sodium chloride crystals usually were grown from molten, reagent-grade NaCl by the Bridgman technique.[15] The doped "laboratory-grown" samples, denoted by an L prefix to the sample number, were prepared by adding the impurity to the reagent-grade NaCl. Crystals from several other sources were also used: In particular, sample $B1A$ was "natural rocksalt" from Baden, Germany; sample $H3A$ was grown by the Harshaw Chemical Company, and sample $D1A$ was

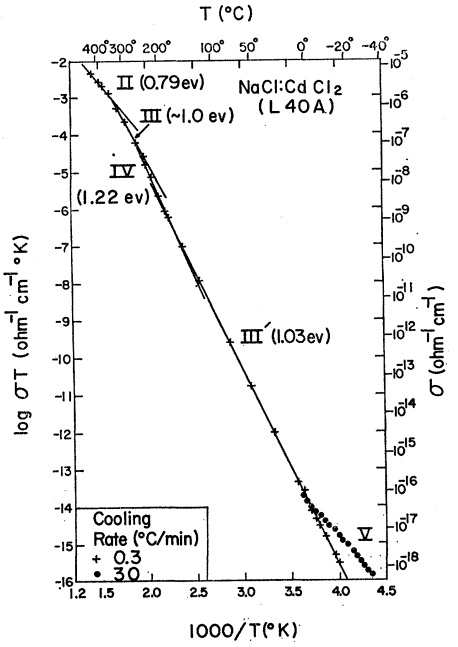

FIG. 2. The conductivity plot of an NaCl:$CdCl_2$ sample, showing the various regions and their slopes.

doped by diffusing Mg ions into a Harshaw crystal at elevated temperature (~770°C). The amount of metallic impurity was determined by semiquantitative spectroscopic analysis and is listed in column 2 of Table I. The sample size (~1×1×0.04 cm) and the electrode material were the same as before.[14]

The sample chamber was the same as described previously.[14] The sample temperature could be varied from −100° to +500°C in this chamber, although the entire range was only occasionally utilized. The temperature, which could be controlled either manually or electronically, was determined to an accuracy of ±0.1° ±0.005T (°C) using either a Chromel-Alumel or copper-Constantan thermocouple.

In the present set of experiments, a tubing connection to the sample chamber was used to introduce nitrogen gas at roughly −100° to −150°C. The cold nitrogen was used when it was desired to cool the samples rapidly from a starting temperature in the range +70° to 300°C down to −70°C. Cooling rates of 20 to 50°C/min were produced in this manner. After rapid cooling, temperatures below ambient were maintained by the use of a one-liter, liquid-nitrogen chamber attached to the top of the sample chamber. One could obtain a cooling rate of 5°C/min starting at 200°C by the use of this one-liter liquid-nitrogen chamber alone.

The electrical current conducted by the sample was measured with a Keithley, model 610, vacuum tube input electrometer. For the work below room temperature, a potential of 250 v was applied to the sample in order to produce an electrical field of about 6000 v/cm. In the vicinity of 40°C, the potential applied to the

[10] A. Joffé, *The Physics of Crystals* (McGraw-Hill Book Company, Inc., New York, 1928).
[11] P. Sutter, thesis, Yale University, 1959 (unpublished); P. Sutter and A. S. Nowick (to be published).
[12] G. Jaffé, Ann. Physik **16**, 249 (1933).
[13] Von Seelen, Ann. Physik **29**, 125 (1924); J. Gingold, *ibid.* **50**, 633 (1928).
[14] R. W. Dreyfus, Phys. Rev. **121**, 1675 (1961).
[15] A detailed description of the sample preparation and equipment has been previously given in reference 14; therefore, only the general features will be reported here. The same numbering system is used here as in reference 14, so that relaxation and conductivity data for the same sample may be compared.

TABLE I. Samples studied and their effective activation energies in the various regions of the conductivity plot.

Impurity (radius in Å)	Impurity conc. (ppm)	Sample number	ϵ_{II} (ev)	ϵ_{III} (ev)	Previous[a] cooling rate in region IV	ϵ_{IV} (ev)	$\epsilon_{III'}$ (ev)
Mg (0.65)	~100	*L48A*	0.80±0.05	···	R	···	0.94±0.04
					S	1.26±0.03	0.90±0.08
	45±7	*L49A*	0.70±0.09	0.97±0.05	R	···	0.92±0.04
					S	···	0.94±0.03
	725±140	*D1A*	···	···	R	···	1.15±0.03
					S	1.28±0.05	1.01±0.05
	130±20	*L70A*	···	···	···	···	···
Mn (0.80)	200±8	*L33B*	0.70±0.10	0.96±0.10	R	···	1.05±0.04
					S	1.10±0.10	0.96±0.04
	360±20	*L33E*	···	0.97±0.10	R	···	1.01±0.03
					S	1.28±0.06	1.04±0.05
	340±20	*L33G*	···	···	R	···	1.05±0.04
					S	1.19±0.08	1.05±0.04
Cd (0.97)	770±160	*L40A*	0.79±0.04	1.0 ±0.1	S	1.22±0.08	1.03±0.03
	1400±100	*L40B*	···	···	R	···	1.03±0.05
			···	···	S	1.31±0.08	1.03±0.04
Ca (0.99)	100±30	*L20A*	···	0.98±0.04	R	···	1.06±0.04
					S	1.23±0.10	1.04±0.04
	2000±600	*L64A*	···	0.92±0.10	R	···	1.01±0.05
					S	1.16±0.10	0.92±0.05
Sr (1.13)	86±49	*L66A*	0.83±0.06	···	S	1.19±0.06	1.12±0.06
	~80	*L66C*	···	···	S	···	···
Ba (1.35)	340±100	*L51A*	···	···	R	···	1.11±0.04
					S	1.27±0.04	1.07±0.05
	~300	*L51D*	···	1.18±0.04	S	1.32±0.10	1.17±0.05
Harshaw	<10	*H3A*	0.82±0.05	···	R	···	1.09±0.02
					S	1.33±0.02	1.01±0.04
Pure	<100	*L19A*	0.75±0.10	1.03±0.03	R	···	1.04±0.01
					S	1.18±0.03	0.99±0.04
Pure	<100	*L31A*	0.80±0.10	1.07±0.05	S	1.29±0.05	1.09±0.03
Pure	Recrystallized	*L63*	···	···	···	···	···
Natural	~100	*B1A*	0.83±0.03	···	···	···	···

[a] R = rapidly cooled (>3°C/min); S = slowly cooled (<1°C/min).

sample was reduced to 67 v and at about 100°C it was further reduced to 9 v. In all of the present experiments, the behavior of the crystals was found to be ohmic as has been previously reported.[11,14]

The data for conductivity vs temperature were taken with the temperature increasing, unless otherwise noted.

3. RESULTS AND DISCUSSION

A typical conductivity curve, showing the various regions seen in the present set of experiments, is given in Fig. 2 for a crystal doped with $CdCl_2$. This figure covers the temperature range from above 400°C down to −35°C, and a conductivity range of thirteen decades. Each region is labeled with the value of the effective activation energy obtained from the slope of the plot. The intrinsic range, region I, was not usually observed in these experiments, since the specimen chamber was not designed to exceed a temperature of 500°C. This deficiency is not serious, however, since region I has been investigated thoroughly by several previous workers who have made conductivity measurements almost to the melting point. As stated in the Introduction, one of the major objectives of the present measurements was to explore the possibility of observing a quenched-in state, where the degree of vacancy-impurity dissociation is greater than the equilibrium value, and therefore the conductivity is enhanced. The solid circles in Fig. 2 show that such an effect is indeed present in samples "quenched" at about 30°C/min from about 150° to −60°C (region V). Figure 2 also shows that the quenching effect has disappeared by the time the rapidly cooled sample is brought above 0°C. In order to understand this quenching effect and the manner of its annealing, it is first desirable to understand the nature of the various regions which are observed at the higher temperatures, i.e., above about 10°C. Accordingly, Sec. 3(a) will first deal with our observations on those regions,

before going on [in 3(b)] to be a detailed investigation of the quenched state.

a. Conductivity Behavior above 10°C

The conductivity curve divides itself up into rather distinct regions, as is shown schematically in Fig. 1 and demonstrated for a specific crystal in Fig. 2. Curves similar to Fig. 2 with σ displaced downward by factors of 10 to 100 were also obtained for "pure" lab-grown crystals. The specific characteristics observed in each region will now be discussed individually and the corresponding experimentally determined activation energies will be compiled in Table I.

Region II. Column 4 of Table I lists the experimentally determined activation energies, ϵ_{II}, for the various crystals studied. The present results for ϵ_{II} are in agreement with the values generally found by others for the slope in this region (see Table II). From Table II we obtain an average value for ϵ_{II} of 0.80 ev. As discussed in the Introduction, region II is usually interpreted in terms of the presence of a temperature-independent concentration of sodium-ion vacancies, n, which is determined by the content of divalent cation impurity. Based on this interpretation, ϵ_{II} should be equal to the activation energy, ϵ_m, for motion of a cation vacancy. The fact that the values of ϵ_{II} given in Table I do not show any systematic dependence upon the radius of the impurity ion (which are listed in the first column) is in agreement with this interpretation.

Region III. Region III is the conductivity region beginning at the low-temperature end of region II where the slope increases rather abruptly. This change in slope, which occurs in the range between 300° and 400°C for doped samples and near 250°C for "pure" samples, is illustrated in Fig. 2 and in the upper curves of Fig. 3. Region III terminates in another abrupt increase in slope corresponding to an increase in ϵ by about 0.2 ev. The extent of this region varies considerably among different samples and for different cooling rates. Figure 4 illustrates the conductivity for a sample doped with

TABLE II. Activation energy, ϵ_{II}, and frequency factor, ν_0, as derived from conductivity data of various authors in region II.

Author	ϵ_{II} (ev)	$\nu_0(10^{14}\ \text{sec}^{-1})$[a]
Bean[b]	0.78±0.02	1.4
Etzel and Maurer[c]	0.85[d]	2.0
Biermann[e]	0.81	1.5
Kobayashi and Tomiki[f]	0.74	···
Dreyfus and Nowick (present work)	0.80±0.03	0.7

[a] In computing the value of ν_0 from each author's data, the conductivity value selected was one at the high-temperature end of region II, in order to be sure that association does not enter. Also, the value of ϵ_m used was the best value reported here, rather than the value of the individual author given in Table II.
[b] C. Bean, thesis, University of Illinois, 1952 (unpublished).
[c] See reference 6.
[d] This value is not actually ϵ_{II} but is obtained by analysis of data for the concentration dependence of the conductivity.
[e] W. Biermann, Z. physik Chem. **25**, 90 (1960).
[f] K. Kobayashi and T. Tomiki, J. Phys. Soc. Japan **15**, 1982 (1960).

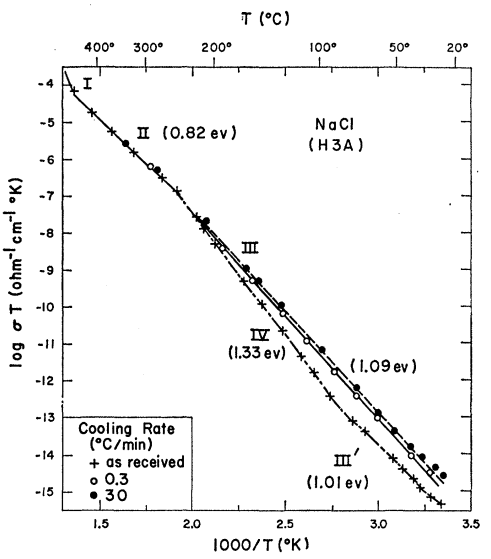

FIG. 3. The conductivity plot for a Harshaw crystal as received, and subsequent to various cooling procedures.

$CaCl_2$, where region III covers over four decades in conductivity and terminates at about 150°C. On the other hand, in Fig. 2, region III extends for less than one decade in σT.

Column 5 of Table I lists values of ϵ_{III} obtained from data for those samples having conductivity curves where the length of region III is sufficient for a definite slope to be measured. In the Introduction, two mechanisms were recognized that could give rise to a steepening of the conductivity curve below region II. These are: (1) association of cation vacancies with divalent impurity ions, and (2) precipitation of the impurity ions. Since it will be shown below that region IV is correlated

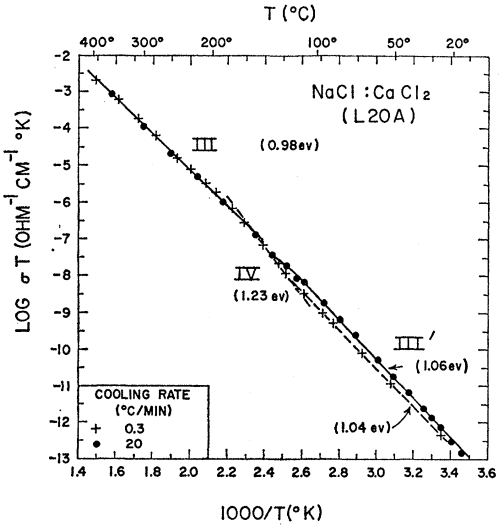

FIG. 4. The conductivity plot for an NaCl:$CaCl_2$ sample, showing the essential absence of region IV after the sample has been rapidly cooled from 300° to 20°C, and its presence after slow cooling.

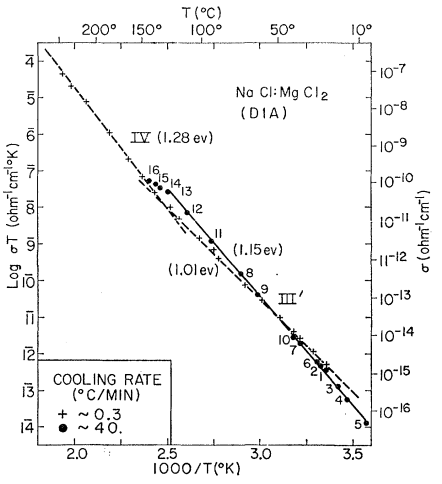

FIG. 5. A conductivity plot showing the effect of slow and rapid cooling upon a heavily doped NaCl:$MgCl_2$ sample. The sequence of measurements on the rapidly cooled sample is indicated by the numerals 1–16.

with the occurrence of precipitation, we are led to conclude that region III results from association. Also, the fact that no hysteresis occurs in region III suggests that precipitation is not involved in this region. Finally, substitution of the theoretically calculated value[7,8] $\epsilon_A \approx 0.4$ ev and the measured value $\epsilon_m = 0.8$ ev into Eq. (11) gives $\epsilon_{III} \approx 1.0$ ev. The rough agreement of this value with the measured values indicates the correctness of the notion that region III is controlled by association.

Region IV. As already mentioned, region III of the conductivity curve terminates with another increase in slope to a value corresponding to $\epsilon \sim 1.2$–1.3 ev; this will be termed region IV. Figures 2–4 show that region IV is observed (on heating) in the range between 100° and 200°C, for samples which had been cooled relatively slowly to room temperature. The measured values of ϵ_{IV} are listed in column 7 of Table I. Rapid cooling (at about 20–30°C/min) of doped samples from about 300°C to room temperature virtually eliminates the appearance of this region, as is shown in Fig. 4, while in the "pure" sample even slower cooling will suppress region IV (see Fig. 3). Similar results were found for NaCl:$CdCl_2$, but these are not shown in Fig. 2 because the large range covered makes the additional data difficult to illustrate graphically.

In the case of rapidly cooled samples, indicated by the solid circles in Fig. 4, an instability was noted near 150°C during the time necessary to make the measurements, whereby the conductivity tends to decrease with time. This instability is well illustrated in Fig. 5 by the points numbered 13 through 16. It is evident that as long as the temperature of the rapidly cooled sample did not exceed 80°C, the conductivity at lower temperatures was reproducible. However, the 2-hr time interval between points 13 and 16 at temperatures near 130°C resulted in a noticeably decreased conductivity, with the points approaching the conductivity curve for the slowly cooled sample.

A reasonable interpretation of region IV is that the divalent-cation impurity ions, which are precipitated to form a second phase in the slowly cooled sample, begin to redissolve during the measurement of the conductivity curve above 100°C. The strongest confirmation of this suggestion comes from the fact that other techniques[8,16,17] show that precipitates redissolve in the temperature range between 100° and 200°C. Direct confirmation of the redispersing of precipitates was also obtained for some of the present samples by visual observation. In crystals containing roughly 100–1000 ppm of $CdCl_2$, $BaCl_2$, or $MnCl_2$, the precipitate phase in slowly cooled samples scattered sufficient light so as to produce a hazy appearance. When such crystals were reheated to a temperature of 200°–250°C, they were observed to become completely transparent. This observation thus confirms that a second phase is present in slowly cooled samples and that it redissolves below 200°C. The absence of region IV, and the correspondingly higher conductivity values of rapidly cooled samples, is presumably the result of the prevention of precipitation because of the rapid cooling. Such samples then show an instability when heated to about 150°C, where precipitation can begin to occur at a reasonable rate. In terms of this interpretation, the effective activation energy, ϵ_{IV}, is equal to that for region III, plus a term which depends on heat of solution of the precipitate.[1]

Region III′. Since region IV is due to the precipitation reaction, which ceases to occur at reasonable rates below 100°C, one can expect a continuation of region III below this temperature. In order to distinguish this new region of the conductivity plot from the higher temperature region III, we shall call this region III′. Indeed, a slope is observed in the range below 100°C which has a value similar to that observed in region III.

Region III′ of the conductivity plot extends, with essentially constant slope ($\epsilon_{III'} \sim 1.0$ ev), to the lower limit of conductivity measurements as determined by the sensitivity of the electrometer. As shown in Figs. 2, 4, and 5, this region may be observed over as much as six to nine decades in the conductivity. Because of its length, the slope of region III′ is generally obtained with relatively good precision. Values of $\epsilon_{III'}$ obtained from the slopes are tabulated in the last column of Table I. Two sets of values are listed, corresponding to runs in which the sample was cooled rapidly through region IV prior to the conductivity measurements (designated "R") and those in which it was cooled slowly (designated "S"). The essential equality of ϵ_{III} and $\epsilon_{III'}$ is evidence that the association reaction controls the cation vacancy concentration in region III′ as it does in region III. Figures 3 and 4 also show that when impurity precipita-

[16] T. Ninomiya, J. Phys. Soc. Japan **15**, 1601 (1960).
[17] J. Cook and J. Dryden, Australian J. Phys. **13**, 260 (1960).

tion is suppressed by rapid cooling, regions III and III′ may join together to cover a wide range of conductivity values.

As in the case of region III, the principal experimental facts concerning region III′ can be explained by the simple association theory [Eqs. (6)–(11)] outlined in the Introduction. The only change required for region III′ is that $N_M{}^0$, the total concentration of divalent impurity, should be replaced by $N_M{}^u$, the concentration still unprecipitated in region III′. This interpretation regards the precipitated impurity as completely removed from the lattice, so that it does not contribute to the vacancy concentration or affect the association reaction. In these terms, the different levels of conductivity of slowly and rapidly cooled samples in region III′ are readily understood.

Although the major point concerning region III′ is the similarity of its slope to that of region III, detailed study of many samples shows the following refinements. First, it is found that region III′ is not actually a straight line, but rather that the slope of the plot in the vicinity of 50°C is about 0.05 (±0.02) ev smaller than the slope in the range 5°–20°C. Second, it is observed that rapid cooling of samples from ~300°C to room temperature increases $\epsilon_{III'}$ slightly. This fact may be noted by comparing values of $\epsilon_{III'}$ in Table I for runs designated R and S on the same sample. The effect of this slight change is such that region III′ of the conductivity plot for rapidly cooled samples tends to converge with and sometimes even to cross over the curve for slowly cooled samples near room temperature. A similar effect has also been observed by Cook and Dryden.[17] The most extreme case of this crossing over found in the present work is illustrated in Fig. 5 for NaCl:$MgCl_2$. Somewhat more typical examples are shown in Figs. 3 and 4, in which a barely detectable but real tendency toward convergence is experimentally observed.

In view of Eq. (11), which predicts that for a given divalent impurity the slope in regions III and III′ should be independent of the concentration of the impurity, it is clear that the simple-association theory cannot explain the observed convergence and crossing over of the conductivity plots. This theory also fails to explain the small (0.05 ev) increase in slope of the conductivity plot at the lower temperatures. Further refinements of the theory are clearly necessary in order to interpret these finer points in the experimental results. The most logical step in refining the theory is to introduce higher complexes in addition to the MV type. This problem will be taken up in a later paper.

b. Conductivity of Samples in the Quenched State

Having considered the nature of the conductivity curves for samples above 10°C, we will now proceed to describe experiments concerned with region V, which occurs for quenched samples. For the purpose of the present paper quenching is defined as rapid cooling (~30°C/min) from above 100°C to about −60°C.

In Fig. 2, the solid circles show the conductivity data for an NaCl:$CdCl_2$ sample which had been quenched from 150°C. It should be noted that the electrical conductivity near −20°C has been increased about an order of magnitude as a result of the quenching. Similar experiments on several other pure and doped samples also indicate that σ can be increased by 10 to 100 times at low temperatures by this quenching treatment. It was also determined that using the 1-liter liquid-nitrogen container alone, so as to produce only a 5°C/min cooling rate (see Sec. 2), enhanced σ almost as much as the above quenching treatment. This fact indicated that neither quenching strains nor moisture in the very cold nitrogen gas were responsible for the increased conductivity.

From the above facts, it was tentatively concluded that an increased concentration of dissociated Na^+ vacancies could be frozen into the lattice by quenching, to produce the enhanced electrical conductivity. If this interpretation is correct, one may expect to obtain a value for the activation energy for vacancy motion, ϵ_m, from region V, since the concentration of free-vacancies should be constant within this region, as was pointed out in the Introduction. The preliminary results failed, however, to yield a precise value for the activation energy, because the quenched-in state of enhanced conductivity was not stable (i.e., a partial return to equilibrium was occurring) during the time of approximately two hours necessary to make the series of measurements. This instability was particularly noticeable in the higher temperature portion of this region (above −10°C). To extend the range of measurement by obtaining data at temperatures appreciably lower than −40°C was not practical because of two limitations. First, the sensitivity of the electrometer limited the conductivity range which could be covered. Second, as the sample temperature was changed, a current which was roughly proportional to the rate of temperature change ($\sim 10^{-14}$ amp for $dT/dt = \frac{1}{4}$°C/min), flowed through the sample. This latter effect appears to be primarily due to the increase (~0.04%/°C) in the dc dielectric constant, κ, with increasing temperature.[18] Thus, it is apparent that if the data are taken very slowly, annealing will occur with corresponding instability in σ, whereas for fast heating, a spurious current due to $d\kappa/dT$ will also contribute to the measurement.

The above difficulties were circumvented by making measurements of σ vs T at a constant (but low) heating rate, and by analyzing the curves of $\log\sigma T$ vs $1/T$ in such a way as to take into account the instability of the quenched-in concentration of vacancies. The constant heating rate was attained by supplying an essentially

[18] B. N. Matsonashvili, Bull. Acad. Sci. U. S. S. R. **22**, 296 (1958).

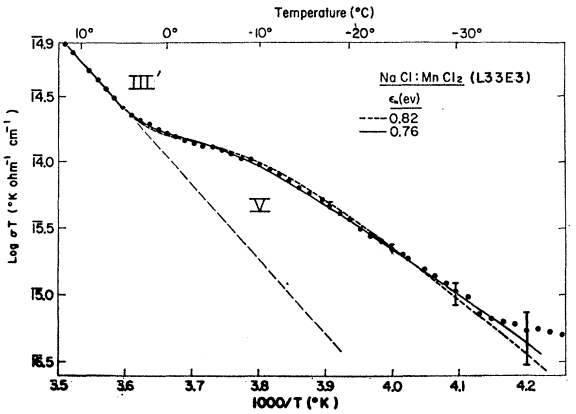

FIG. 6. Typical results for $\log\sigma T$ vs $1/T$ in region V showing both the enhanced conductivity at low temperatures and the elimination of the excess free vacancies near 0°C. The data were taken starting below −40°C and increasing the temperature at 0.224°C/min. Two theoretical curves, for $\epsilon_m=0.82$ and 0.76 ev, are compared to the data.

constant amount of electric power to the thermally isolated sample chamber. Small variations were made in this power level in order to maintain the linear time-temperature relationship. A typical result for region V of the conductivity curve, under the condition $dT/dt=$const, is given in Fig. 6. The method for obtaining the theoretical curves shown in this figure is outlined below.

In order to analyze data such as appear in Fig. 6, it is first necessary to determine the isothermal kinetics for the annealing-out of the enhanced conductivity. Figure 7 illustrates the annealing behavior for Mn^{++} and Mg^{++} doped crystals. This behavior, i.e., the fact that the annealing obeys essentially first-order kinetics, is typical of that observed for doped crystals. Results, such as are shown in Fig. 7, imply the presence of a time-independent number of trapping centers for the excess cation vacancies. This behavior rules out the possibility that the predominant process is the recombination of vacancies with unassociated impurities, since this latter process would involve second-order kinetics.

Several isothermal annealing curves were obtained for one particular sample (*L33B*) in an attempt to determine the activation energy for annealing. The activation energy found was 0.9±0.3 ev; the large error

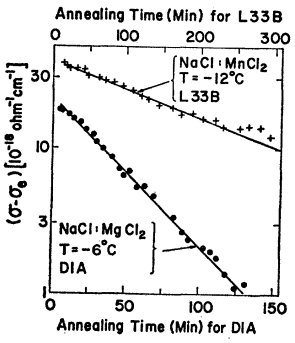

FIG. 7. Isothermal annealing of the quenched-in excess conductivity, showing that the kinetics are first order.

results from the limited range of time (and hence temperature) over which the annealing could be conveniently observed with the present equipment. Also, there was a large amount of scatter in the time constants determined for the annealing; this scatter may have resulted from the inability to reproduce exactly the same number of trapping centers in successive quenching experiments.

As suggested above, measurements within region V of $\log\sigma T$ vs $1/T$ at constant heating rate can be analyzed in terms of the activation energy for cation vacancy motion, ϵ_m. In order to carry out this analysis, we first derive a theoretical expression for the dependence of n upon T. In finding $n(T)$ the experimental fact that first-order kinetics are observed in the vacancy annealing may be expressed as follows:

$$dn/dt=-(n-n_e)/N_j\tau_v. \tag{12}$$

Here, n is the concentration of vacancies at a particular time, n_e is the equilibrium concentration of vacancies at temperature T, τ_v is given in Eq. (2), and N_j is the average number of jumps that a vacancy makes before it is trapped. The assumption that N_j is a constant expresses the fact that the kinetics are first order. Also it is assumed in Eq. (12) that the Na^+ vacancies are migrating to the traps, and not vice versa.

The use of a constant heating rate, $b=dT/dt$, converts Eq. (12) into a one-variable problem, the solutions of which can be expressed as $n(T)$. Appendix I shows how Eq. (12) can be solved exactly for the condition of a constant heating rate, to provide the relation:

$$n(T)-n_e(T)=\left[n_q-\frac{(\epsilon_{III'}-\epsilon_m)}{k}\int_0^T\frac{n_e(T')dT'}{T'^2F(T')}\right]F(T). \tag{13}$$

The quantity n_q is the concentration of quenched-in vacancies, while the function $F(T)$ is given by:

$$F(T)=\exp\int_0^T\frac{-d\theta}{bN_j\tau_v(\theta)}=\exp\left[\frac{12\nu_0}{bN_j}\int_\infty^{1/T}\frac{d(1/\theta)e^{-\epsilon_m/k\theta}}{(1/\theta)^2}\right]$$

$$\approx\exp\left[-\frac{12\nu_0kT^2e^{-\epsilon_m/kT}}{bN_j\epsilon_m}\left(1-\frac{2kT}{\epsilon_m}+\cdots\right)\right]. \tag{14}$$

In the above, Eq. (2) was used to substitute for τ_v.

Although Eq. (13) appears rather complex, the meaning of each of the terms is not difficult to see. The left-hand side of Eq. (13) is the departure of the vacancy concentration from the equilibrium value. The right-hand side is related to the ways in which this non-equilibrium can arise under the present conditions. First of all, the product $n_qF(T)$ is the original, quenched-in vacancy concentration multiplied by a term $F(T)$, which represents the probability that one of these vacancies is still free by the time that the temperature T has been reached. The product of the last term in the brackets

TABLE III. Parameters derived from quenched samples, characterizing the state of greater-than-equilibrium dissociation.

Impurity	Sample	Previous cooling rate in region IV[a]	$[\epsilon_m]_V$ (ev)	N_j/ν_0 (10^{-11} sec)	n_q (10^{15} cm^{-3})	n_e at -25°C (10^{15} cm^{-3})
Mg	*L49A*	S	0.74±0.03	2.7	65	4.7
	L49A	R	0.80±0.03	3.2	89	11.4
	L70A	S	0.85±0.04	3.1	49	4.9
	L70A	R	~0.8	~1.2	~20	14.8
Mn	*L33B*	R	0.78±0.04	>2.3	47	9.7
	L33E	...	0.84±0.03	~5.8	37	9.1
	L33E	S	0.78±0.03	2.3	42	2.8
	L33E	S	0.81±0.03	2.5	36	3.1
Cd	*L40A*	S	0.72±0.08	~0.5	36	3.4
	L40B	S	0.80±0.05	...	34	1.85
	L40B	S	0.83±0.04	...	9.5	~1.4
Ca	*L64A*	S	0.80±0.06	2.4	142	40
	L64A	R	0.83±0.08	1.3	108	22
Sr	*L66C*	S	0.72±0.06	2.45	5.3	0.38
	L66C	S	0.78±0.04	3.2	3.2	0.43
Pure	*H3A*	S	~0.8	~200	~0.02	0.0015
	H3A	R	...	~58	~0.1	0.0055
	L63A	S	~1	~30	0.7	0.025
	L63A	R	...	<3	...	0.054

[a] This column designates whether the sample had been slowly or rapidly cooled through the precipitation range (region IV) immediately prior to it being quenched to −60°C.

and $F(T)$ represents the amount by which the net vacancies generated (due to dissociation) during the finite time of heating to temperature T falls short of the equilibrium number $n_e(T)$. Actually this last product has a relatively small value as compared to the first product on the right-hand side of Eq. (13) in the cases being considered.

The vacancy concentration in Eq. (13) is transformed into conductivity by the use of Eq. (1). The value of $n_e(T)$ is directly related to $\sigma_e(T)$, the equilibrium value of conductivity at temperature T, by the relation $\sigma_e(T)=(An_e/T)\exp(-\epsilon_m/kT)$, where $A=4e^2a^2\nu_0/k$. We also define a quantity $\sigma_q(T_0)$ which is the conductivity immediately after quenching and at a sufficiently low temperature, T_0, that virtually no annealing has taken place. Clearly, this quantity is given by: $\sigma_q(T_0)=(An_q/T_0)\exp(-\epsilon_m/kT_0)$. By means of these relations Eq. (13) can be expressed in a form which is directly comparable to the experimental results, as follows:

$$\sigma(T)-\sigma_e(T)=\frac{e^{-\epsilon_m/kT}F(T)}{T}\left\{T_0\sigma_q(T_0)e^{\epsilon_m/kT_0}-\frac{(\epsilon_{III'}-\epsilon_m)}{k}\int_{1/T}^{\infty}\frac{T'\sigma_e(T')e^{\epsilon_m/kT'}}{F(T')}d\left(\frac{1}{T'}\right)\right\}. \quad (15)$$

The integral appearing in this equation was evaluated as a summation, using the expansion for $F(T)$ given in Eq. (14). For data such as are shown in Fig. 6, $\sigma_q(T_0)$ was chosen so that the theoretical curve and the data agree at a low temperature, such as −25°C. The value of $\sigma_e(T)$, the equilibrium value of conductivity at each temperature T, is found either by an extrapolation of region III′ or by actual conductivity measurements on slowly cooled samples at temperatures down to −15°C.

The two unknown parameters in Eq. (15), which may be obtained by fitting the theory to the data, are ϵ_m and the ratio N_j/ν_0. Fortunately, these two quantities have somewhat different effects upon the theoretical curve, and hence can be effectively separated. The magnitude of ϵ_m essentially controls the slope of the theoretical conductivity curve, for temperatures in the range of −30° to −10°C (see Fig. 6), primarily because of the first factor on the right-hand side of Eq. (15). The parameter N_j/ν_0, on the other hand, is determined primarily by the region of rapid annealing near −5°C.

The procedure used to determine ϵ_m was to compare theoretical curves with $\epsilon_m=0.76$ or 0.82 ev to the conductivity data (in the manner shown in Fig. 6), and to obtain the value which best fitted the data by interpolation (or extrapolation). Since this activation energy is an experimentally derived quantity from the data of region V, it is designated in Table III as $[\epsilon_m]_V$. These results for $[\epsilon_m]_V$ for crystals doped with different impurities show that there is apparently no correlation between the value found for $[\epsilon_m]_V$ and impurity-ion radius. The agreement between the average value, $[\epsilon_m]_V=0.79_6\pm0.02$ ev, and the result from region II ($\epsilon_{II}=0.80\pm0.03$ ev) serves to show that the interpretations involved in analyzing both of these regions are correct. Specifically, it appears reasonable to believe that both ϵ_{II} and $[\epsilon_m]_V$ represent the activation energy

for motion of a cation vacancy. The error of ± 0.02 ev for $[\epsilon_m]_V$ includes both the 0.016-ev standard deviation and a 0.01-ev allowance for systematic errors. Utilizing Eq. (4), together with the best experimental value for ϵ_I and the above value for ϵ_m, we obtain for the energy of formation of a Schottky defect in NaCl, the value: $\epsilon_s = 2.12 \pm 0.07$ ev.

The other parameter determined from the data of region V is N_j/ν_0. The ratio N_j/ν_0 is fitted to the data in the range where this factor has the greatest effect, i.e., in the region of rapid annealing. In Figs. 2 and 6, this rapid annealing is seen to occur in the temperature range around -5°C. The values of N_j/ν_0 which were determined in this way are also listed in Table III. For results similar to Fig. 6, small variations in the value of N_j/ν_0 were found to have little effect upon the theoretical curve below about -10°C; hence the determination of the best value of N_j/ν_0 can be effectively separated from the determination of $[\epsilon_m]_V$. The uncertainty in the value of N_j/ν_0 was estimated to be $\pm 10\%$ unless otherwise indicated in Table III.

Having obtained the ratio N_j/ν_0 from measurements in region V, we note that it would be helpful to obtain separately a value for ν_0 so that the quantity N_j will be determined for the various crystals studied. It is also useful to know ν_0 in order to be able to determine the jump rate of a free cation vacancy at any temperature, in accordance with Eq. (2). The quantity ν_0 cannot be obtained from the data for region V, since the actual value of n_q is not known in this region. On the other hand, it is readily obtained for region II, where $n = N_M^0$ [see Eq. (5)], since N_M^0 may be determined by chemical analysis. Equation (1) shows that ν_0 can be determined, once ϵ_m and n are known, from the conductivity at any one temperature. Values for ν_0 obtained in this way from the data of various authors are listed in Table II. An average result $V_0 = 1.3 \times 10^{14 \pm 0.3}$ is obtained. The scatter in values of ν_0 obtained from the different authors may be due in part to errors in the quantitative analysis, (especially because of the small impurity concentrations involved) and the possible existence of a finite background impurity level. An uncertainty in ν_0 also arises from the uncertainty in ϵ_m. The theoretical significance of ν_0 and its comparison with the frequency factor obtained from dielectric relaxation measurements has been dealt with elsewhere.[4]

It is interesting to compare the value of ν_0 determined from the conductivity to that obtained from combined conductivity and Hall effect measurements by Read and Katz.[19] The latter measurements provide values of mobility in the temperature range 600–780°C. Substituting the measured mobility at a given temperature and $\epsilon_m = 0.79_6$ ev into Eq. (1), one obtains a frequency factor of $2.1 \times 10^{14 \pm 0.1}$ sec^{-1}. Read and Katz have deduced that frequency factors determined by their method should agree with that from conductivity alone within about a factor of 2. They note, however, that just as in the case of semiconductors, the two types of mobility (and hence the values of ν_0) may not be identical.

Having obtained values for ν_0 and ϵ_m, one can now express the mobility of an Na^+ vacancy in NaCl as:

$$\mu(T) = (4800/T) \exp[0.79_6(\text{ev})/kT] \text{ cm}^2 \text{ °K/v-sec.} \quad (16)$$

Using Eq. (16), the values of σ_q and σ_e [used to fit Eq. (15) to the data from region V] may be converted into the corresponding vacancy concentrations, n_q and n_e. Values for these latter quantities are listed in the last two columns of Table III. It should be recalled that n_q is the (nonequilibrium) vacancy concentration present after quenching but before annealing, while $n_e(T)$ is the equilibrium vacancy concentration at temperature T.

Knowledge of the constant ν_0 also makes possible the calculation of the quantity N_j, the number of vacancy jumps involved in the annealing of region V, from the experimentally determined ratios N_j/ν_0 listed in Table III. Detailed examination of the results for N_j will be treated in a later paper, where the nature of the traps which capture the excess free vacancies will be considered. For the present, it suffices to note that values of N_j for doped crystals fall in the range from 1000 to 5000, while for "pure" crystals, values which are one to two orders of magnitude higher are obtained. This result essentially demonstrates that the vacancy traps contain the divalent-cation impurities.

4. SUMMARY AND CONCLUSIONS

The data from the present work provide evidence as to the validity of the following points:

(a). A nonequilibrium excess of dissociated cation vacancies may be quenched into a sample by cooling at rates ~ 30°C/min. This vacancy excess anneals out of the crystal, according to a first-order kinetic equation, in the vicinity of 0°C.

(b). The activation energy, ϵ_m, for cation vacancy motion in NaCl is $0.79_6 \pm 0.02$ ev, while the energy, ϵ_s, to create a Schottky pair is 2.12 ± 0.07 ev.

(c). The presence of association between cation vacancies and divalent-cation impurities results in a steepening of the conductivity plot corresponding to an effective activation energy in the range 0.95 to 1.1 ev. The range in which impurity precipitation can occur reversibly shows an activation energy still higher by about 0.2 ev.

ACKNOWLEDGMENTS

The authors are grateful to F. G. Fumi for many helpful discussions, and to W. R. Heller for his comments on the manuscript. The "laboratory-grown" samples were prepared by K. W. Asai and the spectroscopic analysis was carried out by D. P. Cameron, J. C. Webber, and W. Reuter.

[19] P. Read and E. Katz, Phys. Rev. Letters **5**, 466 (1960); P. Read, thesis, University of Michigan, 1960 (unpublished).

This paper is based in part on a dissertation presented by R. W. Dreyfus for the degree of Doctor of Philosophy at Yale University.

APPENDIX I. ANNEALING OF VACANCIES DURING HEATING AT A CONSTANT RATE

The concentration of vacancies, n, in a quenched sample which is subjected to annealing is a function of time (t), temperature (T), and the annealing history. For first-order kinetics, the instantaneous annealing rate is given by Eq. (12) of the text. Introducing a constant heating rate, $T=bt$, makes $n(t,T)$ become an explicit function of the temperature alone. Equation (12) then becomes:

$$\frac{dn}{dT}+\frac{n}{bN_j\tau_v(T)}=\frac{n_e(T)}{bN_j\tau_v(T)}, \tag{A1}$$

with τ_v given by Eq. (2). It is convenient to solve Eq. (A1) as if the sample is heated starting at 0°K. Thus, n_q is the concentration of quenched-in vacancies (present at $T=0$°K). Since Eq. (A1) is linear, its exact solution is well known:

$$n\exp\int_0^T\frac{dT'}{bN_j\tau_v(T')}=n_q+\int_0^T dT'\frac{n_e(T')}{bN_j\tau_v(T')}\times\exp\int_0^{T'}\frac{dT''}{bN_j\tau_v(T'')}.$$

Integrating the last term by parts, and then using the definition

$$F(T)=\exp\int_0^T\frac{-d\theta}{bN_j\tau_v(\theta)}=\exp\left[\frac{-12\nu_0}{bN_j}\int_0^T d\theta\exp(-\epsilon_m/k\theta)\right],$$

the exact solution for n becomes:

$$n(T)-n_e(T)=\left[n_q-\int_0^T\frac{dn_e(T')}{F(T')}\right]F(T). \tag{A2}$$

The final step in obtaining an expression for $n(T)$ is to express the second integral in the brackets in terms of dT'. To do this, we point out that taking the equilibrium conductivity as the extrapolation of region III′ of the conductivity plot, is equivalent to writing:

$$n_e(T')\propto\exp\left[\frac{-(\epsilon_{III'}-\epsilon_m)}{kT'}\right].$$

Differentiating this relation, provides:

$$\frac{dn_e(T')}{dT'}=n_e(T')\left[\frac{\epsilon_{III'}-\epsilon_m}{kT'^2}\right].$$

Substituting the above relation into (A2), provides the solution for $n(T)$ given in Eq. (13) of the text.